NASA TT F-9811

ELECTRON PROBE MICROANALYSIS OF LIGHT ELEMENTS

R.Castaing and J.Descamps

Translation of "Le dosage des éléments légers par le microanalyseur à sonde électronique". La Recherche Aéronautique, No.63, pp.41-52, 1958.

NATIONAL AERONAUTICS AND SPACE ADMINISTRATION
WASHINGTON DECEMBER 1965

ELECTRON PROBE MICROANALYSIS OF LIGHT ELEMENTS

***/41

R.Castaing* and J.Descamps**

13298

The proportional analysis of light elements in various alloys, cosmic magnetic spherules, and marine sediments by electron probe microanalysis is described, with structural details on the microanalyzer used and photomicrographs of the investigated specimens. The relative accuracy of analysis with the described apparatus is 1% at high concentrations of the elements, permitting a detection of contents as low as 0.02%. The accelerating potential is kept to the minimum compatible with the correct excitation of the characteristic lines of the elements, so as to keep the diffuse penetration of elements in depth within the specimen to a minimum. To prevent atmospheric contamination, the gas pressure was kept slightly above 1 atm. Corrections to be made for absorption and for secondary fluorescence of X-rays within the specimen are formulated. Application of the method is checked on several typical examples, including the Mg_2Si phase in an Al-Mg-Si alloy.

SUMMARY

The point analysis by X-ray emission, its basic characteristics, and its

* University of Paris, member-at-large of the ONERA.

** Research Engineer at the ONERA.

*** Numbers in the margin indicate pagination in the original foreign text.

potentialities were studied in previous publications (Bibl.1, 2). Those papers contain a detailed description of the original apparatus, designed and developed at the ONERA (French National Aerospace Research and Development Administration).

Subsequent studies yielded more detailed data on the physical laws involved in the method and the experimental conditions of its use (Bibl.3).

Two analyzers of a previously designed type were constructed at the ONERA; one was exhibited in June 1955 at the French Physical Society and has been in continuous service at the IRSID since October 1955.

The second analyzer was kept at the ONERA and, in addition to being used in many routine analyses, has also been further improved.

A brief resumé of the principles of a point analysis by emission, will be followed by a description of the modifications made in the method (extension to light elements) as well as on the apparatus itself.

Several examples will be given for demonstrating the various fields of application of the method.

***

The application of X-ray spectrography to the chemical analysis is rather old, since it is more than a half century that the first work done by Moseley has pointed the way. The basic principle is quite simple: A complex specimen is excited by primary bombardment. This will cause it to emit an X-radiation whose spectrum includes mainly the characteristic lines of the various constituent elements. A spectrographic analysis of this emitted radiation will thus directly lead to a qualitative chemical analysis of the bombarded specimen. The extreme simplicity of characteristic X-ray spectra, that comprise only a few

lines, eliminates all risk of ambiguity.

Two different methods can be used for exciting X-ray emission of the specimen: The exciting agent can consist of a primary X-ray beam, which then involves a fluorescence analysis; we were mainly interested in a spectrographic analysis by direct emission, where the X-ray emission of the specimen is excited by electron bombardment.

Since its very beginnings, X-ray spectrography by direct emission has been highly successful. This method has specifically permitted the discovery of new elements: Let us mention only the discovery of hafnium in 1923 by Coster and Hevesy, that of masurium in 1925 by Noddack, Take, and Berg, and many others.

However, some difficulties are encountered when attempting to convert this analytical method into a method of quantitative determination. For this, the procedure used to be as follows: Assume that the concentration of an element A in a mixture - generally in the form of powder - was to be determined. First, the intensity is determined at which the mixture, under well-defined electron bombardment conditions, emits the most important characteristic line of the element A. After this, increasing quantities of a control element B are introduced into the mixture, which element has an atomic number close to that of the element A. This is continued until the mixture emits the homologous characteristic lines of the elements A and B at the same intensity. It is then assumed that the concentration of the element A is equal to that of the control element B. It is immediately obvious that this method of quantitative analysis, in addition to its complexity, is quite inaccurate, since it is actually founded on a comparison of the intensities of two X-radiations of different wavelengths. These two radiations are absorbed in different manners by the specimen, by the exit window of the tube, and by the air; they are reflected at a different efficacy for the

monochromator crystal; finally, they are recorded at a different sensitivity by the receiving element of the spectrograph. The ratio of intensities read from the spectrograph thus differs greatly from the ratio of intensities actually emitted by the specimen; this makes it necessary to introduce uncertain corrections that basically depend on the equipment used. In fact, it is practically impossible to compare, in an absolute manner, the intensities of the two X-ray emissions unless these radiations have the same wavelengths. This particular statement formed the basis for development of the point analysis method (Bibl.1, 2, 4) whose principle will be briefly reviewed here.

An electron probe (extremely thin electron beam) is directed on a point /42 of the surface of a solid specimen whose chemical composition is to be studied. The very small volume of matter irradiated by the electrons, of the order of one square micron, emits, under the impact of this electron bombardment, an X-radiation that comprises the characteristic lines of the various elements present at the point of impact of the probe. A spectrographic analysis of this radiation, in a very simple manner, then permits obtaining the respective concentrations of these various elements at the analyzed point.

For example, let us assume that the concentration of nickel at a certain point of a given specimen is to be determined. This point is brought to impact with the electron probe; the spectrograph is aligned with the line $NiK\alpha_1$, and the recorded intensity is noted in arbitrary units. Then, without touching the adjustment of the electron beam or that of the spectrograph, the specimen under the probe is replaced by a pure nickel block and the new intensity recorded by the spectrograph is noted. The ratio of the two readings will furnish an excellent approximation of the nickel concentration at the analyzed point.

This especially simple result can be derived directly from Webster's law

(Bibl.1, 3) according to which the progressive loss of energy of the electrons along their path in the matter depends essentially on the density of the material traversed, which is more or less independent of its chemical composition. This law has been experimentally verified in all analyses made at the ONERA on homogeneous specimens of known composition. The main reason for this simplicity lies in the absolute nature of the measurements: The radiations, whose intensity is being compared, have the same wavelength, and all difficulties that might

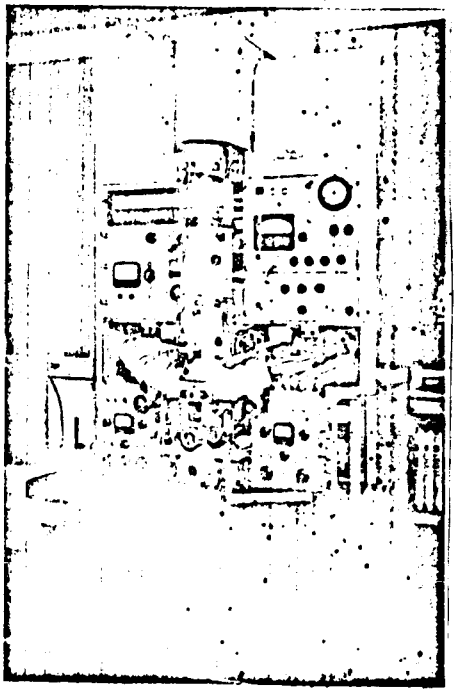

Fig.1 Overall View of the Microanalyzer

originate from the absorption of the radiation or from the yield of the spectrograph are automatically eliminated, because of the fact that they enter the two terms of the ratio to the same extent. The quotient of the two readings (disregarding for the time being the absorption in the specimen itself, to which we will return later) furnishes an accurate ratio of the total emissions, in the analyzed line, of both specimen and pure element. This ratio has an intrinsic

importance, independent of the experimental equipment used. The absolute character of this analytical method makes all comparison with control alloys, of a composition similar to that of the specimens, unnecessary; such a comparison is conventional in optical spectrography. Such an absolute character is indispensable for a practical utilization of the method, since it would be impossible to obtain an entire range of homogeneous test alloys on a small scale.

To give a general idea on the performance of the apparatus, let us mention that the relative accuracy of the proportional analysis is of the order of 1% at high concentrations. It becomes less good at low concentrations (5%, for a concentration of the order of 1%). At the critical limit and in favorable cases, it is possible to detect contents of the order of 0.02%.

The resolving power (minimum diameter of the region in which an accurate quantitative analysis is possible) is about 2μ, where the limit is given by the diffuse penetration of the electrons into the matter. However, a qualitative analysis is possible for much lower diameter heterogeneities, at the limit of resolution of ordinary light microscopes.

The experimental equipment described in an article in the Recherche Aéronautique, No.23 (1951) had the basic function of studying the fundamental laws and the potentialities of the method. It was soon found that the diversity of the problems that can be studied by this method necessitated the construction of a more flexible microanalyzer of greater potentiality and useful for non-specialized research.

This apparatus, of which two prototypes were developed at the ONERA (Fig.1) will be described below.

1. Overall Structure of the Analyzer (Fig.2)

The apparatus comprises the following four principal elements:

a) an electron lens system, which is to produce the probe;

b) a metallographic microscope (aligned with the analyzed point);

c) a mechanical unit permitting the displacement of the specimen and of the pure-element controls under vacuum;

d) a battery of spectrographs for analyzing the emitted X-radiation.

The main drawback of the original apparatus was the poor quality of the device for visual display of the specimen. This consisted simply of an ordinary microscope objective, in front of which a mirror was placed at an angle of 45° between the object and the last reducing lens. The mirror was pierced with a hole for allowing passage of the electron beam, and considerations of bulk limited the aperture ratio of the objective to about 0.2. It is quite obvious that the quality of the images furnished by the viewing device is insufficient under such conditions. In fact, the investigator must be able to detect structural details of a given specimen with the same ease as under a high-quality metallurgical microscope.

Therefore, the viewing conditions had to be greatly improved. The solution used by us consisted in eliminating the mirror and in directly observing the /43 specimen by means of an objective coinciding with the axis of the electron beam. However, this solution has not always been found practical since it involves a basic modification of the entire apparatus, specifically a replacement of the electrostatic lenses of the original analyzer by magnetic lenses (Fig.3).

a) Production of the Probe

The probe is produced by an electron gun with tungsten filament and HF heating, followed by two magnetic lenses which give a reduced image of its crossover.

The first lens has a focal length which is variable between 2 mm and infinity. This lens plays the role of a condenser, and adjustment of its excitation permits the formation of probes with diameters between 0.1 and 10 μ.

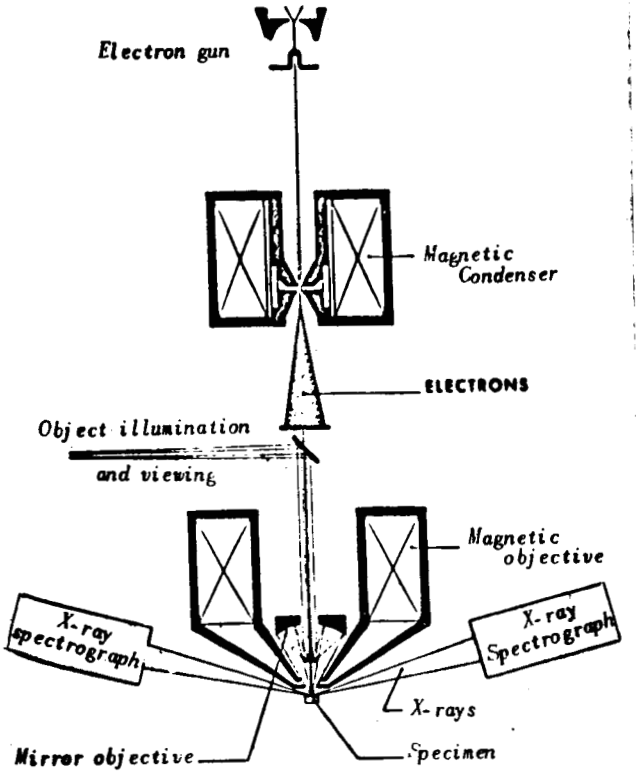

Fig.2 Schematic Principal Diagram

The second reducing lens produces an accurate convergence of the electron beam at the surface of the specimen (focal length: about 9 mm; formation point of the probe, 6 mm below the lower face of the pole pieces).

An electrostatic device permits a correction of the residual astigmatism of this lens as well as minor lateral displacements of the probe, so as to compensate the slight deviations occasionally produced in an analysis of magnetic specimens.

We have found that the introduction of a highly magnetic specimen into the apparatus may lead to displacements of the probe as great as 10 μ. Such dis-

placements would not interfere if it were merely a question of marking the analyzed point; observation of the "contamination" spot forming on the specimen after bombardment of a few minutes, actually permits a strict localization of the impact point of the probe. However, a displacement of the impact point, due to magnetism of the specimen, might lead to a minor distortion of the spectrograph, which in turn would lead to an error of measurement.

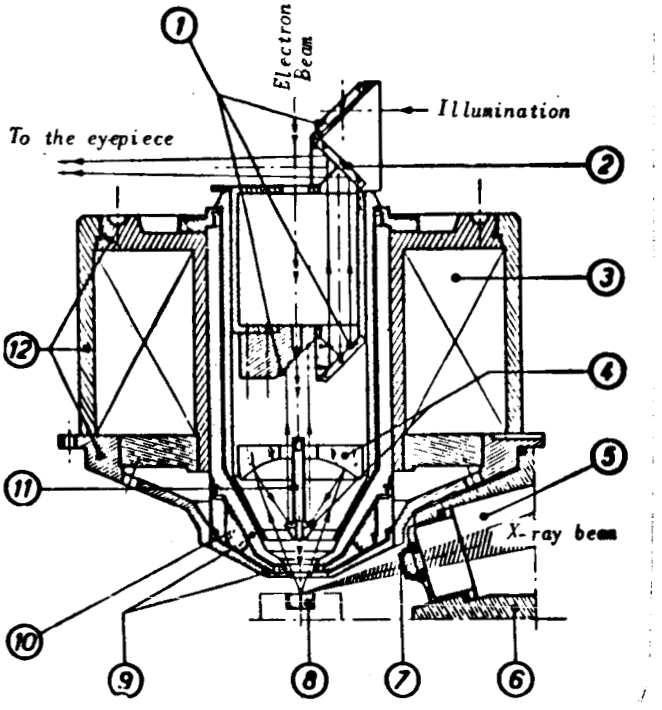

Fig.3 Schematic Sketch of the Objective Lens
1 - Mirrors; 2 - Semisilvered section; 3 - Winding; 4 - Mirror objective; 5 - X-ray spectrograph in air, in primary vacuum, or in secondary vacuum; 6 - Casing; 7 - Exit window, adjustable during operation; 8 - Object; 9 - Pole pieces; 10 - Electrostatic astigmatism corrector; 11 - Electrostatic shielding; 12 - Body

Therefore, it is of importance, before taking any intensity reading, to have the impact point of the probe coincide with the crosshair and, if necessary, to obtain such coincidence by manipulating the astigmatism corrector.

An aperture diaphragm, fixing the aberrations of the objective lens to a

suitable value, permits a compromise between the two contradictory requirements, namely, obtaining a minimum diameter for the probe and a maximum intensity for the electron current carried by this probe.

It is also of considerable importance to select the lowest possible value for the accelerating potential, compatible with a correct excitation of the characteristic lines of the analyzed elements. In fact, the diffuse penetration of electrons into a given element increases with their energy, and a high resolving power requires that this penetration be kept to a minimum.

The high potential obtained by commutating a HF voltage (75 kc), can be /44 fixed to seven values, staggered from 10 to 35 kv and adjusted to within a few hundred thousandths.

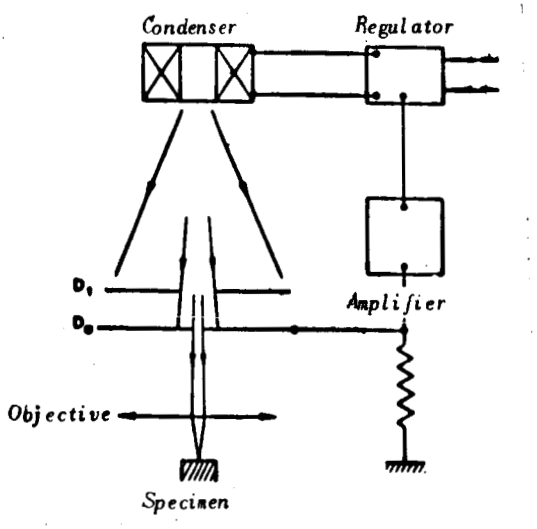

Fig.4

The feed of the two magnetic lenses is intensity-stabilized by an electron process, using a battery of cells. A possible variation in the resistance of the windings during heating of the lens thus has no effect on the magnetizing current. This is a prerequisite for preventing any deviation in the focal length of the lenses.

Adjustment of the electron beam. Some difficulty may be created by the fact that the electron current transported by the probe somewhat varies during protracted experiments.

This electron current has recently been made independent of possible variations in total emission of the gun, by introduction of a control device. This regulator is schematically shown in Fig.4. The aperture diaphragm D_0 of the second reducing lens is preceded by a coaxial diaphragm D_1 with a k times greater diameter. It is immediately obvious (since the electron density in the plane of the diaphragm D_1 is uniform near the center) that the diaphragm D_0 thus receives an electron current I correlated with the current i, transported by the probe, by the very simple relation: $I = (k^2 - 1)i$.

Thus, main emphasis must be placed on ensuring constancy of the current I. This is obtained by grounding the diaphragm D_0 across a high resistance: The potential of this diaphragm (several volts below the ground) is used for obtaining excitation of the condenser.

The regulation is sufficiently efficient to ensure that a variation in total emission of the gun from single to double will not entrain a variation greater than 1% of the electron output of the probe.

b) Viewing Microscope

The objective of the metallurgical microscope, during the experiment, must permit an observation of the specimen and a localization of the impact point of the probe on its surface.

In addition, the objective must meet the following requirements:

a) large image distance, while maintaining suitable magnification and adequate relative aperture;

b) pierceability along its axis, to permit passage of the electron beam;

c) absence of nonconducting surfaces that might acquire electrostatic charges;

d) absence of optical surfaces with respect to the probe, at short length. These surfaces would rapidly become "contaminated" under the action of the diffuse electrons.

Use of a mirror objective offers a simple solution of this problem.

The objective used here is of the type developed by Nomarski, who was in charge of mounting and adjusting the objective at the Optical Institute. This objective consists of two concentric spherical mirrors. Its characteristics are as follows: focal length, 12 mm; image distance, 17 mm; numerical aperture, 0.48; resolving power, $\sim 0.7\ \mu$.

The illumination of the specimen was based on the principle developed by Köhler.

A special wide-field ocular (formula by C.Zeiss) was provided with a reticle, interrupted near the center, and with a filar micrometer whose individual divisions correspond to 2 microns on the specimen. The magnification of the microscope is 400 ×.

c) Displacement of the Object and Controls

The object carrier and 42 samples consisting of pure elements or wanted combinations are placed on a rigid cartridge, which slides out from the vacuum enclosure of the apparatus (2×10^{-5} mm Hg) through two flexible vacuumtight membranes.

A unit of exterior slide bars permits a displacement in height (focusing of

the viewing microscope) and movements in two rectangular directions in the focal plane. These motions are controlled by graduated knurled drums.

With this arrangement, it is possible to successively place the point selected for analysis, and later the pure control element, at the impact point of the electron beam. In addition, the arrangement also permits - before starting the analysis - placing a small fluorescent screen underneath the beam, carrying a polished copper block on which the contamination spots appear. This permits a fine adjustment of the focal length of the magnetic objective and exact coincidence of the impact point of the probe with the object.

d) Spectrographs

For an analysis of the X-ray emission from the object, two spectrographs with cambered crystal and counter are used. Both crystal and counter rotate on the same focusing circle of 25 cm radius. A gear train makes it possible to give the counter a rotational speed twice that of the crystal. In this manner, the radiations reflected by the crystal, no matter what the selected angular position and thus no matter what the reflected wavelength might be, can be accurately focused on the center of the entrance window of the counter. A dial, graduated in degrees and minutes, permits a constant reading of the angle of incidence of the X-ray beam on the crystal and thus also of the reflected wavelength. The reproducibility of this angle of incidence is better than one minute. For example, it is possible, with the electron beam cut, to align the spectrograph in advance with one or the other of the two components of a doublet $K\alpha_1$ - $K\alpha_2$. It is obvious that, under such conditions, no ambiguity exists as /45 to the nature of the recorded line.

The right-hand spectrograph (Fig.5) is designed for detecting radiations of

medium wavelength, comprised within the band 0.6 Å - 4.5 Å. Thus, by their K lines, this spectrograph permits an analysis of all elements located in the periodic table between chlorine and molybdenum and, by their L lines, of all elements heavier than molybdenum. The counter used is a Geiger-Müller counter sealed with a mica window. The crystal of the spectrograph is a quartz foil of 3/10 mm thickness, cut on the Johannson system.

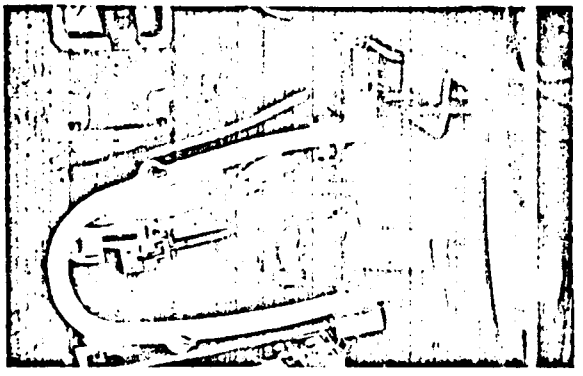

Fig.5 Photograph of the Right-Hand Spectrograph, Open

The left-hand spectrograph (Fig.6) deserves a more detailed description. This spectrograph is designed for detecting very soft radiations, of a wave-

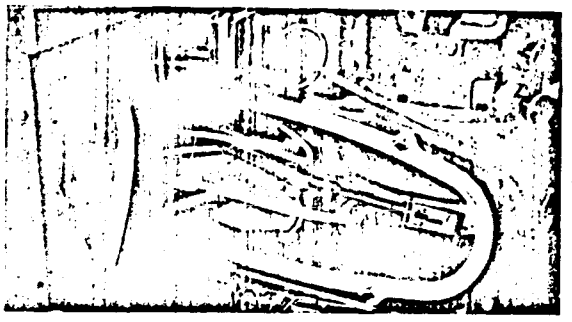

Fig.6 Photograph of the Left-Hand Spectrograph, Open

length between 4 Å and 10 Å. The reflector consists of a curved mica foil of 0.50 cm radius. The receiving element consists of a proportional counter with gas filling (Fig.7). The window of this counter is a mylar foil of 6μ thickness

whose absorption is only about 40% for a radiation as soft as $SiK\alpha_1$ (7.11 Å). A beryllium foil of the same absorption would have to have a thickness of 20 μ. Under these conditions, it would be practically impossible to make this window vacuumtight. The mylar itself is slightly permeable to water vapor, which makes a sealed counter impossible. Consequently, the counter is made detachable and

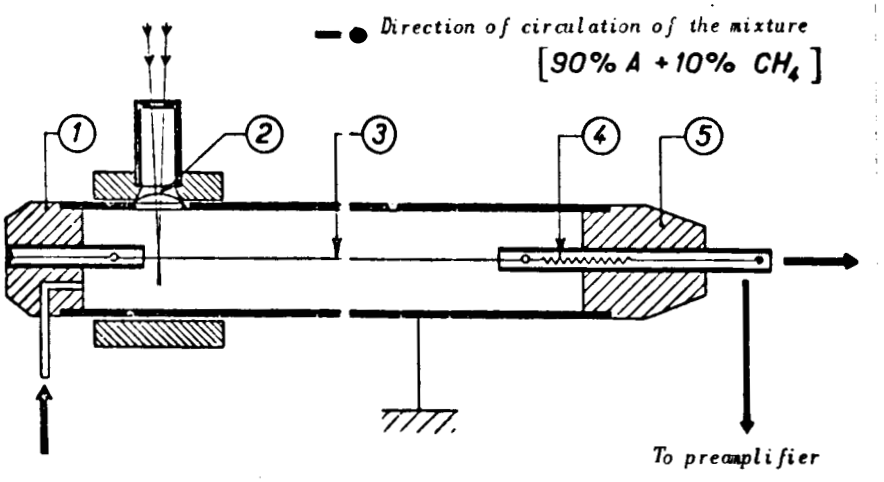

Fig.7 Schematic Diagram of the Proportional Counter
Symbols: 1 - Araldite; 2 - Window (mylar 6 μ); 3 - Tungsten wire (20 μ); 4 - Spring for wire tension; 5 - Araldite

is traversed by a gas current. The rate of flow of the gaseous mixture (90% argon + 10% methane) is about 10 cm^3/min. The lateral arrangement of the window makes it possible to avoid a dead spot which always is encountered in counters with end windows. The drop in sensitivity of the counter from the side of long wavelengths thus is due exclusively to the absorption of the window which is negligible up to 10 Å. A valve system (Fig.8) permits placing the counter under vacuum before introducing the gas. This prevents the long evacuation which would otherwise be necessary to completely remove the air from inside the counter, and makes the device ready for operation within less than 5 min. The constancy of gas output is ensured by a capillary.

The operating pressure of the gas is slightly above 1 atm, which prevents any contamination by atmospheric air; the small diameter (20 μ) of the center tungsten wire permits a reduction in the operating voltage to 1500 v. A pre-amplifier, placed into the vacuum of the spectrograph, follows the counter in

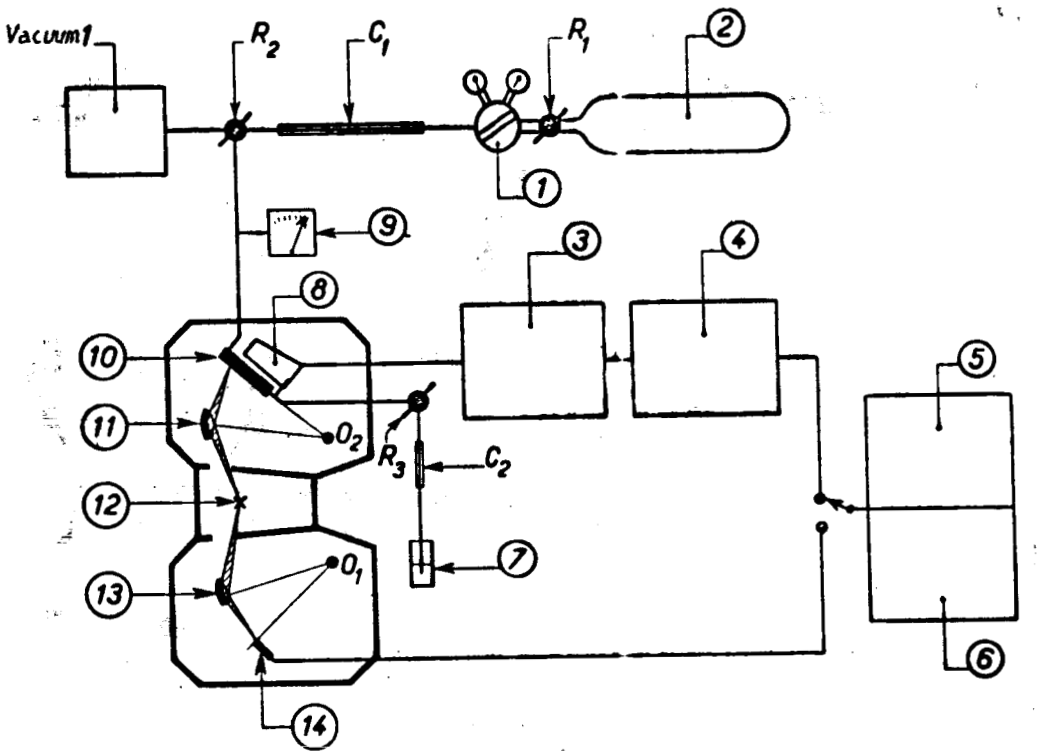

Fig.8 Schematic Diagram of the Spectrographs and Gas Filling of the Proportional Counter
Symbols: 1 - Pressure reduction valve; 2 - Compressed gas (90% A + 10% CH_4); 3 - Linear amplifier; 4 - Amplitude selector; 5 - Pulse counter + integrator; 6 - High-voltage feed of the counters; 7 - Output meter; 8 - Preamplifier; 9 - Pressure gage for the counter; 10 - Proportional counter; 11 - Mica; 12 - Probe; 13 - Quartz; 14 - Geiger-Müller counter

all its displacements. The pulses are fed to a linear amplifier, provided with an amplitude selector, which permits a considerable improvement in contrast of the line against the continuous background.

To give a general idea, let us mention that the $SiK\alpha_1$ line emitted by a block of 746

pure silicon, for an electron bombardment with an accelerating potential of 15 kv and an intensity of 0.1 μamp (probe of 1 micron), presents an intensity of about 1000 discharges/sec, which is entirely sufficient for a rapid and accurate measurement. Naturally, it is necessary to place the spectrograph under vacuum for recording such soft radiations. Any penetration of atmospheric air into the spectrograph would reduce the intensity of the $SiK\alpha_1$ line, by absorption, at a ratio of 10^{13}! To avoid the use of an absorbing screen between the source and the counter, a secondary vacuum is produced in the spectrograph and the beryllium exit window is eliminated. Such a beryllium window of 8/100 mm thickness, intersecting the beam, is sufficient to reduce the intensity of the $MgK\alpha_1$ radiation by a factor of 140.

In this manner, after having selected a region to be analyzed of 1 micron diameter on a given specimen, the electron probe can be accurately focused on this region, and the intensity of the various characteristic X-rays, emitted for a small volume of 2 μ diameter around the investigated point, can be measured with high accuracy.

The analysis proceeds as follows:

One starts with a qualitative analysis, which is readily obtained by having the spectrographs sweep their entire wavelength domain. The various elements, present in the analyzed volume, will show in a high reflected intensity for the wavelengths of their characteristic lines.

This is followed by a quantitative analysis. For this purpose, after adjusting the spectrograph to an intense line of one of the elements present, the reflected intensity is noted as the number of pulses per second in the counter. If necessary, the resultant figure is corrected to take the "dead time" of the counter into consideration and to allow for the continuous background (eigen-

motion of the counter and continuous X-ray spectrum). At the focus of the probe, the specimen is replaced by a control block consisting of the pure element. The ratio of the two measurements, in first approximation, will yield the concentration of the element in question at the analyzed point. The measurement itself is greatly facilitated by the permanent presence of a set of controls in the analyzer, consisting of the principal elements in their pure state.

This permits a proportional analysis, either from their K lines or from their L lines, of all elements having an atomic number above or equal to 12 (magnesium), contained in the specimen. The restriction to magnesium has its reason in the geometry of the spectrograph used and in the reflecting crystal, i.e., the mica. It would also be possible to eliminate this, but this would render the analysis of very light elements highly unreliable due to the absorption of X-rays in the specimen itself, a point we will discuss in more detail below.

e) Miscellaneous Corrections /47

We mentioned above that the concentration of a given element in a complex anticathode is more or less equal to the ratio of intensities emitted (in the characteristic line of this element) by the anticathode and by a control block of the pure element. This holds true, however, only if the actually emitted intensities are considered, i.e., corrected for their absorption in the anticathode itself, no matter whether the specimen or the control block are involved. Consequently, it would be useful to apply a correction to the measured intensities, known as a correction for absorption, so as to obtain the true emissions of which the ratio can then be formed.

Let I be the intensity recorded by the spectrograph in a certain character-

istic line of wavelength λ; let θ be the exit angle of the analyzed beam, and μ/ρ the mass absorption coefficient for this line of the analyzed region of the specimen.

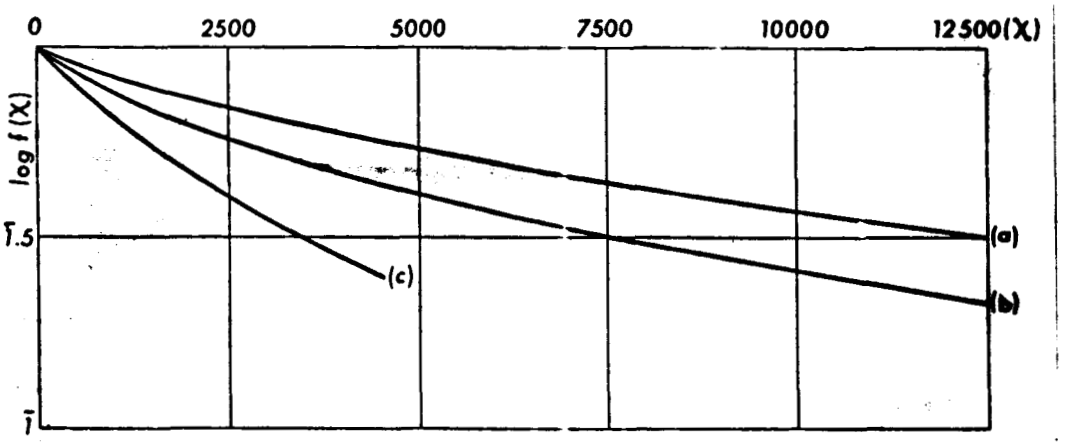

Fig.9 Correction Curves for Absorption, for V = 9.7 kv; 15.1 kv; 27.5 kv
a - V 9.7 kv - $\bar{Z}$ = 13; b - V 15.1 kv - $\bar{Z}$ = 13;
c - V 27.5 kv - $\bar{Z}$ = 26

Let I_o be the intensity actually emitted at the interior of the specimen, i.e., the intensity which would be recorded by the spectrograph if no X-ray absorption were present.

The ratio $\frac{I}{I_o}$ can be expressed in the form of $\frac{I}{I_o} = f(\chi)$, where χ = $= \mu/\rho \operatorname{cosec} \theta$. The form of the function f depends mainly on the accelerating potential.

Figure 9 gives three correction curves for absorption, which correspond to the accelerating potentials 9.7 - 15.1 - 27.5 kv. On the abscissa, the argument $\chi = \mu/\rho \operatorname{cosec} \theta$ is laid off, while the ordinate gives the logarithm of the ratio $\frac{I}{I_o}$.

In principle, a determination of these correction curves requires a complete and detailed study of the distribution in depth of the characteristic emis-

sion of the various anticathodes, for an accelerating potential given by the exciting beam; no quantitative experimental data are in existence on this distribution. The obtained experimental results were reported in an article published in the Journal de Physique (Bibl.3).

However, one can rather rapidly obtain a correction curve, without going over the intermediary of the distribution in depth of the X-rays. The procedure consists in measuring the variation in emitted intensity, as a function of the exit angle θ of the radiation (Bibl.1). The correction to be applied can be directly read from the curve. This curve, for a given accelerating potential, is valid for all wavelengths and all reflection angles. It depends very little on the nature of the anticathode, and one single curve can be applied for all specimens, so long as lines of relatively short wavelength are used, to keep the correction small. To give a general idea, let us mention that, for the characteristic lines of elements heavier than titanium, the absorption correction generally does not exceed 10%. This is no longer the case for light elements, where the correction may reach 50% and thus must be determined with extreme care.

It is then no longer possible to assume that the form of the function f is independent of the type of specimen; thus, for an accurate determination of the correction for absorption, the "mean atomic number" $\overline{Z}$ of the absorbing medium must be taken into consideration. For this reason, we indicated the mean atomic number of the anticathode, used in the determination, on the three curves a, b, c of Fig.9. An impression of the influence of the mean atomic number on the slope of the correction curve for absorption can be obtained by referring to Fig.10 which, for various anticathodes and equal accelerating potential, gives the curves for the absorption correction, obtained from an experimental determi-

nation of the distribution in depth of the characteristic X-radiation.

A brief examination of the curves in Fig.9 indicates that, in the case of light elements in which values of χ of 5 - 6000 are quite common, it is preferable to use a low accelerating potential for the electron beam, i.e., 15 kv or even 10 kv. It is obvious that the penetration of the electrons into the specimen will then be much less and the absorption of the X-ray beam will be greatly

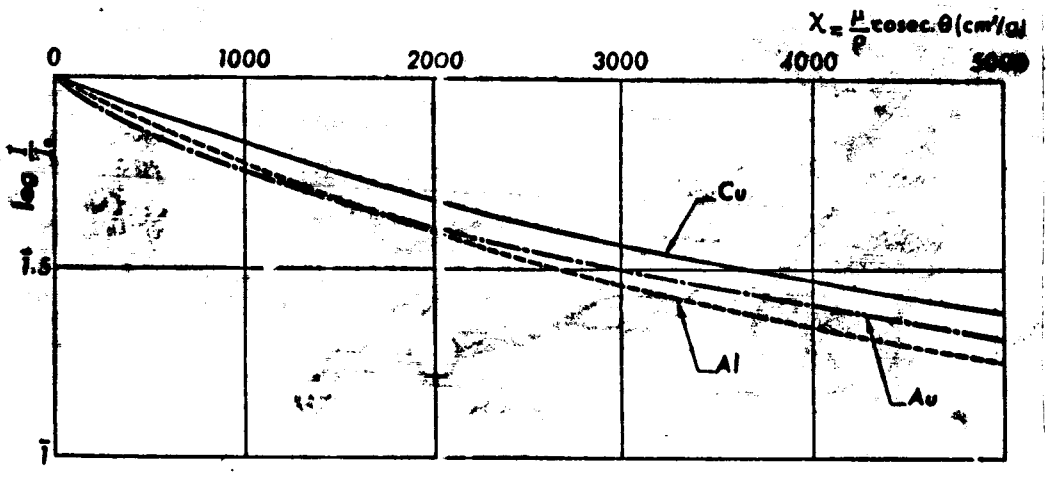

Fig.10 Correction Curves for Absorption, at V = 27.5 kv
Experimental Points, absorbents: Al - Cu - AU

reduced. This still does not do away with the fact that the absorption within the specimen is the main reason for the inaccuracy in analyzing light elements. This absorption may reach 50% in adverse cases and, which is even much more serious, depends greatly on the angle of exit of the beam. However, this exit angle which is about 18° in our apparatus and would be accurately known if the specimen were rigorously plane, can be locally modified by an amount of the /48 order of one degree. This is the case, for example, in the analysis of a precipitate which always shows as a slight elevation or a minor depression after mechanical polishing. It therefore is suggested to apply careful polishing and to make use of electrolytic polishing, specifically for alloys consisting of light elements, where the latter process is highly attractive for convenience

reasons.

Finally, a second correction is necessary because of the fact that the characteristic radiation emitted by the specimen is partly due to secondary fluorescence phenomenon. In addition to the primary radiation, produced by direct

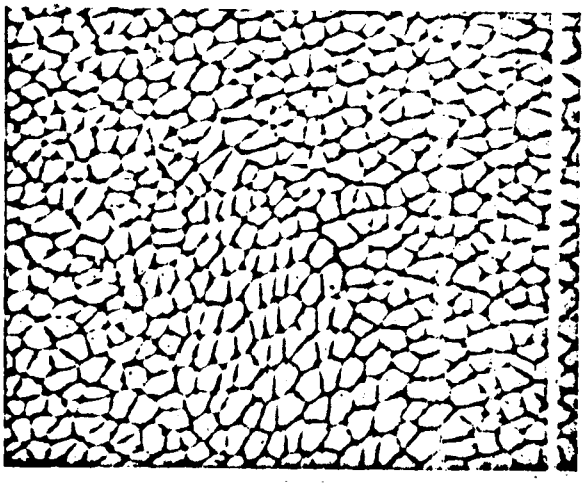

Fig.11 Alloy AlMn (1.25% Mn); 225 ×

excitation of the atoms of the specimen by the electron beam, a fluorescence radiation is created by atoms excited by the primary X-radiation (characteristic lines and continuous spectrum). Correction formulas were established (Bibl.1, 3) that permit an almost complete elimination of this error source.

2. Typical Applications

The point analysis method by X-ray emission has been successfully applied to specimens of widely differing types. Naturally, metallurgy is the most important field of application; however, the analysis can also be extended to include insulating materials that merely need be given a thin metallic coating by vacuum deposition, so as to make them surface-conducting. In mineralogy as well as in biology, this opens a practically unexplored field of application. The

use of this method will be briefly described on hand of some typical analyses made with the ONERA apparatus.

1) Al-Mn Alloy

The Al-Mn alloy with 1.25% of manganese, rough-cast and rapidly quenched, exhibits a cellular structure (Fig.11). On the request of Mrs.M.K.B.Day (British Aluminum Company), we investigated the distribution of manganese in this particular alloy.

We were able to prove a significant difference between the manganese content at the centers of the various cells (1.12% Mn ± 0.02%) and the content along the edges (1.27% Mn ± 0.03%).

A similar segregation was recorded for an alloy with 1.08% Mn average content.

2) Al-Cu-Fe Alloy

The ternary system Al-Cu-Fe is little known at present; the ternary phase has a poorly defined existence domain. Various formulas were proposed by different authors: The main ones to be cited are the formulas of Al_6Cu_2Fe by Hanemann and Schrader; $Al_{12}Cu_4Fe$ by Wiehr; Al_7Cu_2Fe by Phragmen (Bibl.5); Yamaguchi and Nakamura were able to identiyy two phases: Al_6Cu_2Fe (ψ) and Al_7Cu_2Fe (ω).

A rapid analysis made it possible to eliminate the formula $Al_{12}Cu_4Fe$. A more refined quantitative analysis was necessary for selecting between the formulas Al_6Cu_2Fe (36.9% Cu, 16.15% Fe, 46.95% Al) and Al_7Cu_2Fe (34.16% Cu, 14.96% Fe, 50.88% Al).

In the investigated specimen (prepared by R.Graf of the ONERA) shown in Fig.12, we found 34.8% copper and 14.2% iron on the average, with a scattering

of ±3%.

The analysis, made first for the elements copper and iron, made it seem logical to adopt the formula Al_7Cu_2Fe. The proportional analysis of aluminum yielded no additional data. In addition, this method is much less accurate than that of iron and copper, because of the extensive correction for absorption to be made. In the present case, in which $\overline{Z} = 26$, our absorption curve (estab- /49 lished for $\overline{Z} = 13$) does not permit an accurate calculation of the correction for absorption.

Fig.12 Al - Cu - Fe; 500 ×

3) Cosmic Magnetic Spherules

On the request of Prof.K.Fredriksson (Mineralogiska Institutet, Stockholm), we analyzed magnetic spherules of 50 - 60 μ diameter, obtained from deep marine sediments (red clay of the Pacific and manganesiferous crust), using our apparatus.

We encountered two types of particles: The one type had a nucleus of a metallic appearance (30 μ diameter) surrounded by oxides, while the other was totally composed of oxides.

In the first type, a quantitative analysis indicated that the constituent elements of the nucleus were iron (68%) and nickel (30%), with a minor content of cobalt (1.5%). In the layers surrounding the nucleus, the iron was present at a high concentration (61 - 70%), while the nickel and cobalt concentrations were only of the order of 0.1 - 0.2%.

The outer layer of these particles consists of magnetite, which most likely was formed at the expense of the nucleus, in the marine sediment. In the second type of particles, the nickel content decreases from the center (20 - 24%) to the edge (< 0.5%), while the iron content increases from 40 - 57% at the center to more than 70% along the edges. The boundary is formed of magnetite Fe_3O_4, mixed more or less intimately with FeO; the center, at least for one of these particles, seems to correspond to the formula $NiFeO_4$ ("trevorite").

The oceanographic interpretation and a detailed discussion of this analysis will be published later by R.Castaing and K.Fredriksson (Bibl.6).

4) Marine Sediments

Another specimen had its origin in the deep-sea sediments of the Pacific and was sent to us by Prof.G.Arrhenius (Scripps Institute of Oceanography, LaJolla, Calif.).

This specimen, in the form of powder, contained silicious skeletons of diatoms and radiolaria, phillipsite microcrystals, and yellow aggregates of a roundish form (5 - 15 μ) containing inclusions of a crystalline appearance. An analysis of a large number of isolated particles indicated that the barium content in the diatoms and radiolaria was low (0 - 2%), while that in the phillipsite crystals was distinctly higher (3 - 15%). In the aggregates, we encountered a greatly variable concentration, but always with high maxima(2 - 47%).

Apparently, this barium is present in the form of baryta microcrystals, irregularly distributed within the aggregates.

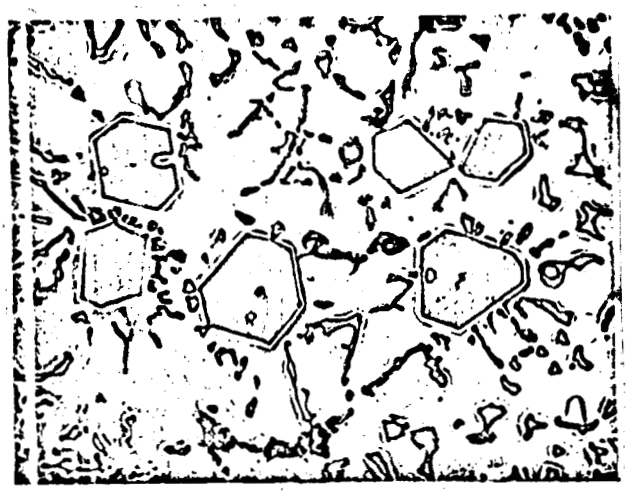

Fig.13 Al-Mg-Si Alloy (Mg_2Si Phase); 300 ×

The origin of these crystals will be discussed in a general investigation of the chemistry of the pelagic sediments of the Pacific, by E.D.Goldberg and G.Arrhenius (Bibl.7).

5) Mg_2Si Alloy

To check on the applicability of our method to light elements, we analyzed the well-known Mg_2Si phase, present in macrocrystals of polygonal cross section, in a rough-cast and slowly tempered alloy Al-Mg-Si (Fig.13).

The accelerating potential was set to 9.7 kv, and the intensity of the beam was 0.2 μamp. The contrast of the lines against the continuous background was about 100.

The following results were obtained:

Si	Mean of experimental results	37%
	Extreme values	35.8 to 38.2%
	Theoretical value	36.8%

Mg	Mean of experimental results	63.5%
	Extreme values	60.6 to 66%
	Theoretical value	63.2%

The absorption correction for the $SiK\alpha_1$ line, excited by electrons of 9.7 kv, is quite extensive (excitation of the K level of magnesium), namely, 55% in relative value. We were able to determine this with accuracy, since the "mean atomic number" of the Mg_2Si phase was practically identical with that of the specimen (pure aluminum) used for constructing the correction curve for absorption.

The correction for fluorescence of the $MgK\alpha_1$ line, excited by $SiK\alpha$, is minor (1.2% in absolute value).

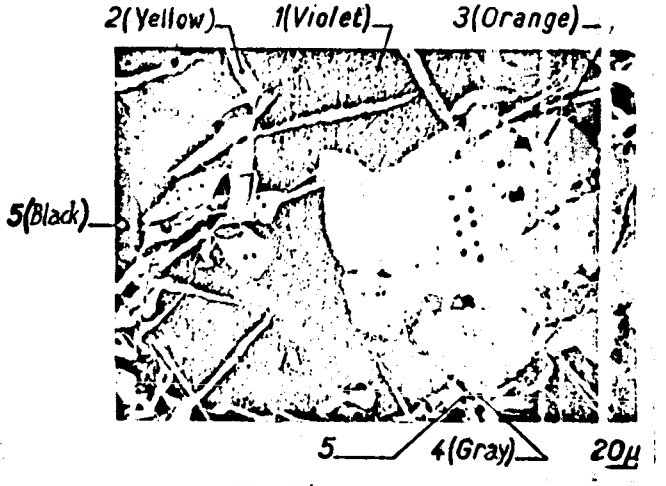

/50

Fig.14 200 ×

6) Complex Sulfurs of Iron and Copper

A proportional analysis of light elements is specifically of importance to the mineralogist, since these are the most widely distributed elements in minerals.

A sulfurized mineral of iron and copper was analyzed.

The metallographic structure of the specimen showed five principal phases (Fig.14):

a bluish violet principal phase (No.1);

a more or less dark yellow phase, in needles (No.2);

an orange phase, in coarse blocks of low number and rounded shape (No.3);

a gray phase, of variegated color (No.4), located at the contact point with the yellow phase;

a black phase (No.5), in polygonal blocks with rounded angles.

The purpose of the analysis was manifold:

1) Check tests on the composition of the phases Nos.1 and 2, which had been identified with bornite (Cu_5FeS_4 or 3 Cu_2S, Fe_2S_3 depending on the authors) and with chalcopyrite ($CuFeS_2$) respectively, by the conventional methods of mineralogy.

2) Heterogeneity of these phases.

3) Qualitative analysis of the three other phases, specifically for detecting Al, Si, Ge, Sb.

4) Quantitative analysis of these three phases for their identification.

The results given in the accompanying Table were obtained.

It should be noted that these figures on the sulfur content are rather uncertain, not so much because of a particular difficulty in analyzing this element but because of the fact that difficulties were encountered in preparing a control specimen of sufficient homogeneity, with an accurately known sulfur content. A control of pure sulfur is difficult to use since the probe-induced local heating of the sulfur, because of its very low heat conductivity, is sufficient to greatly increase its vapor tension and to lead to a rupture of the thin metallic protective conducting layer.

The violet phase is readily identified with bornite whose most often cited empirical formulas are as follows:

$\{ Cu_2FeS_4$ (63,4 % Cu — 11,1 % Fe — 25,5 % S)
$\{ 3\ Cu_2S, FeS_2$ (56.5 % Cu) — 16.6 % Fe — 26.9 % S)

The yellow phase is chalcopyrite, having the formula

$CuFeS_2$ (34.7 % Cu — 30.5 % Fe — 34.8 % S)

with a somewhat higher sulfur content.

In the orange phase, the presence of a high content of tin makes us believe that a stanniferous bornite is involved here. The outer appearance of this mineral has been described elsewhere under the name "orange bornite" (Bibl.8,9).

PHASES	Cu %	Fe %	S %	*Other Elements*	*Elements Present in Low Concentration*
Violet (N° 1)	51-66.2	11.?-15.6	~ 20-30	—	Al, Si, Ge < 1 %
Yellow (N° 2)	30.2-34.7	29.7-35.4	~ 40	—	—
Orange (N° 3)	36.2-44.6	11.4-12	~ 40	Sn 9-10 %	
Gray (N° 4)	41.4-54	3-4	~ 40	As 21 %	Sb ≠ 0
Black (N° 5)	—	—	—	Si ~ 30 %	

The gray phase presents zones of more or less dark coloration. Presumably, we are here in the presence of a variant of tennantite where the Cu_2S content would be low and the As_2S_3 content high. The general formula ($4\ Cu_2S$, As_2S_3) actually is applicable to a series of variants where the ratio of the individual constituents is variable.

The presence of 3 - 4% of iron is not improbable. In analytical tables of these phases, various authors gave values of 0.6% - 3% - 4% and even 5.5%, depending on the specimens involved.

The black phase could not be identified. Qualitatively, we only found silicon as element with an atomic number higher than 11. Since we did not know

what other very light element or elements were present in this particular phase, we can only give an approximate estimate of the silicon content, since it is impossible to accurately calculate the necessary absorption correction. Our mineralogists believe that quartz is definitely involved here. /51

In the extremely complex deposit, from which this particular specimen was taken, it must a priori be expected that various aberrant mineralogical species would be encountered; a detailed investigation on this item is in progress, in collaboration with mineralogists of the Office of Geological, Geophysical, and Mining Research (Lévy).

BIBLIOGRAPHY

1. Castaing, R.: Doctor Thesis. Publication O.N.E.R.A., No.55, Paris, June 1951.

2. Castaing, R.: La Recherche Aéronautique, No.23, pp.41-50, 1951.

3. Castaing, R. and Descamps, J.: Journal de Physique et le Radium, Vol.16, pp.304-317, 1955; C.R., Vol.237, p.1220, 1953.

4. Castaing, R. and Guinier, A.: Proceedings of the Conference on Electron Microscopy. Delft, 1949.

5. Phragmen: J. Inst. Metals, Vol.77, p.489, 1950. (The article contains earlier bibliography).

6. Castaing, R. and Fredriksson, K.: Geochemical and Cosmochemical Acta (to be published).

7. Goldberg, E.D. and Arrhenius, G.: Geochemical and Cosmochemical Acta (to be published).

8. Orgel, J. and Riviera-Plaza, G.: Bull. Soc. Franc. Minéralogie, Vol.51, p.230, 1928.

9. Lévy, C.: Bull. Soc. Franc. Miné. Crist., No.79, pp.383-391, 1956.

Received January 23, 1958